Atmospheric and Oceanic Science Letters 18 (2025) 100587

Contents lists available at ScienceDirect

Atmospheric and Oceanic Science Letters

journal homepage:
http://www.keaipublishing.com/en/journals/atmospheric-and-oceanic-science-letters/

Evaluation of surface wind speed over East Asia and the adjacent ocean in three reanalyses using satellite and in-situ observations

Siyuan Li[a], Kai Wang[b], Hao Miao[c,*], Xuedan Zhu[a], Yanjie Liu[d], Jinxiao Li[a], Wei Wang[a], Xiao Zheng[b], Juan Feng[e], Xiaocong Wang[d,*]

[a] Shanghai Investigation, Design and Research Institute Co., Ltd., Shanghai, China
[b] College of Atmospheric Science, Nanjing University of Information Science and Technology, Nanjing, China
[c] China Meteorological Administration Transportation Meteorology Key Laboratory, Nanjing Joint Institute for Atmospheric Sciences, Nanjing, China
[d] State Key Laboratory of Numerical Modeling for Atmospheric Sciences and Geophysical Fluid Dynamics, Institute of Atmospheric Physics, Chinese Academy of Sciences, Beijing, China
[e] Center for Monsoon System Research, Institute of Atmospheric Physics, Chinese Academy of Sciences, Beijing, China

ARTICLE INFO

Keywords:
Surface wind speed
ASCAT
Reanalysis
Trend analysis
East Asia

关键词:
地表风速
ASCAT
再分析产品
趋势分析
东亚地区

ABSTRACT

Surface wind speed (SWS) not only plays a crucial role in regulating the Earth's energy and hydrological cycle, but also is an important source of sustainable renewable energy. This study assesses the credibility of SWSs in three reanalyses (ERA5, MERRA2, and JRA-55) in East Asia using both satellite and in-situ observations. Results show all three reanalyses can capture the spatial pattern of SWS as in observations, yet there are notable differences in magnitude. On land, ERA5 and MERRA2 overestimate the SWS by about 0.6 and 1.5 m s^{-1}, respectively, whereas JRA-55 underestimates it. The biases over the oceans are opposite to those on land and are relatively small due to the assimilation of observations of oceanic surface winds. Overall, JRA-55 and ERA5 offer better estimates of seasonal means and variances of SWS than MERRA2. The observed SWS shows a negative trend of −0.08 m s^{-1}/10 yr on land and a positive trend of 0.09 m s^{-1}/10 yr in the western North Pacific. Only JRA-55 shows similar trends to observations over both land and ocean, while ERA5 and MERRA2 show varying degrees of deviation from the observations. Further investigation shows that there is a strong link between the trend of SWS and that of the large-scale circulation, and that a large part of the SWS trend can be attributed to changes in large-scale circulations.

摘要

利用卫星和地面站点观测数据, 本文对再分析产品中的地表风速 (SWS) 进行了可信度评估. 研究结果表明, 再分析产品能够较好地再现SWS的观测分布特征, 但在风速的量级上则存在显著差异. 具体而言, 在陆地区域, ERA5和MERRA2分别高估了约0.6 m s^{-1}和1.5 m s^{-1}, 而JRA-55则存在低估现象; 而在海洋区域, 偏差情况与陆地相反. 总体来看, JRA-55和ERA5在模拟SWS的气候态及其变率方面, 更加接近观测数据. 其中, JRA-55中SWS的年代际趋势与观测数据最为一致.

1. Introduction

The wind speed near the surface (10 m) plays a crucial role in influencing surface evaporation and sensible heat flux, and its importance in regulating the Earth's energy and hydrological cycle can never be overestimated (Zheng et al., 2009). Additionally, surface wind is an important kind of sustainable renewable energy resource, which is being rapidly developed around the world due to its safety, cleanliness, and abundance (Fischedick et al., 2011). As a result, there is a growing need to understand and accurately represent surface winds, which is essential to assist in a wide range of applications such as weather forecasting and renewable energy assessment (Vishnu and Francis, 2014; Wu et al., 2018; Miao et al., 2020; Goutham et al., 2021).

Due to the lack of long and homogeneous records of wind speed observations on a global scale, reanalysis products have been widely used as a proxy for assessing wind resources (Cannon et al., 2015; Ramon et al., 2019; Minola et al., 2024; Das and Roy, 2024; Torralba et al., 2017). While reanalysis products provide a comprehensive record of meteorological fields on a global scale, they are inevitably subject to a degree of uncertainty caused by physical parameterizations of the assimilation models (Miao et al., 2019; Wang and Zhang, 2024). On the other hand, remote sensing observations from satellites equipped

* Corresponding authors.
E-mail addresses: miaoh@cma.gov.cn (H. Miao), wangxc@lasg.iap.ac.cn (X. Wang).

https://doi.org/10.1016/j.aosl.2024.100587
Received 9 October 2024; Revised 25 November 2024; Accepted 12 December 2024
Available online 16 December 2024
1674-2834/© 2025 The Authors. Publishing Services by Elsevier B.V. on behalf of KeAi Communications Co. Ltd. This is an open access article under the CC BY-NC-ND license (http://creativecommons.org/licenses/by-nc-nd/4.0/)

with onboard scatterometers provide unprecedented information, from which surface winds can be retrieved. The wind retrievals are typically based on the inversion of the Geophysical Model Function, an empirical model which describes the dependency of the backscatter on ocean wind speed and direction as well as other parameters related to the viewing geometry (Ricciardulli and Manaster, 2021). Numerous studies have been conducted by comparing scatterometer wind speeds with in-situ buoy wind speeds, and good agreement has been found between the two (e.g., Ray et al., 2022; Dickinson et al., 2001).

While many previous studies have used in-situ observations to assess land surface winds in reanalyses, few studies have assessed ocean wind resources, which are typically larger than those over land. The objective of this study is to assess the credibility in surface wind speed (SWS) in three reanalyses in East Asia using satellite and in-situ observations, and to determine which aspects of surface winds in the reanalyses are credible and which are not. In the following, Section 2 describes the datasets and methodology used; Section 3 evaluates the seasonal means and variances of land and ocean surface winds in East Asia; Section 4 compares the trends of SWS between reanalyses and observations, and discusses the extent to which this trend can be attributed to large-scale circulations; and the main findings are summarized in Section 5.

2. Data and methodology

The observed wind speeds on land were obtained from Daily Climate Data from Chinese Surface Stations (V3.0), which includes 6-hourly values from 824 Chinese ground stations. The observations of SWS over the ocean were obtained from the Advanced Scatterometer (ASCAT) onboard Meteorological Operational satellite A, which includes daily values of SWSs with a horizontal resolution of 0.25° × 0.25°. Specifically, we used the version of ASCAT-A (V.2.1.1), which corrected small calibration issues experienced after 2016 (Ricciardulli and Manaster, 2021).

The three reanalyses investigated in this study are the fifth generation ECMWF reanalysis (ERA5; Hersbach et al., 2020), the second Modern-Era Retrospective Analysis for Research and Applications (MERRA2; Gelaro et al., 2017), and the Japanese 55-year Reanalysis (JRA-55, Kobayashi et al., 2015), with horizontal resolutions of 0.25°×0.25°, 0.5°×0.625°, and 1.25°×1.25°, respectively. The time period of all reanalyses spans from March 2007 to October 2021 over the ocean, and from January 1980 to December 2016 over land, thus enabling a maximum overlap between reanalysis products and observations. To facilitate comparisons between different datasets, all observation and reanalysis datasets were extrapolated and processed into daily averages.

3. Seasonal means and variances of SWS

3.1. SWSs over China

Firstly, we compare the seasonal means of SWSs from the reanalyses against in-situ observations over China. The left two columns of Fig. 1 show the spatial distribution of the observed SWS in winter and

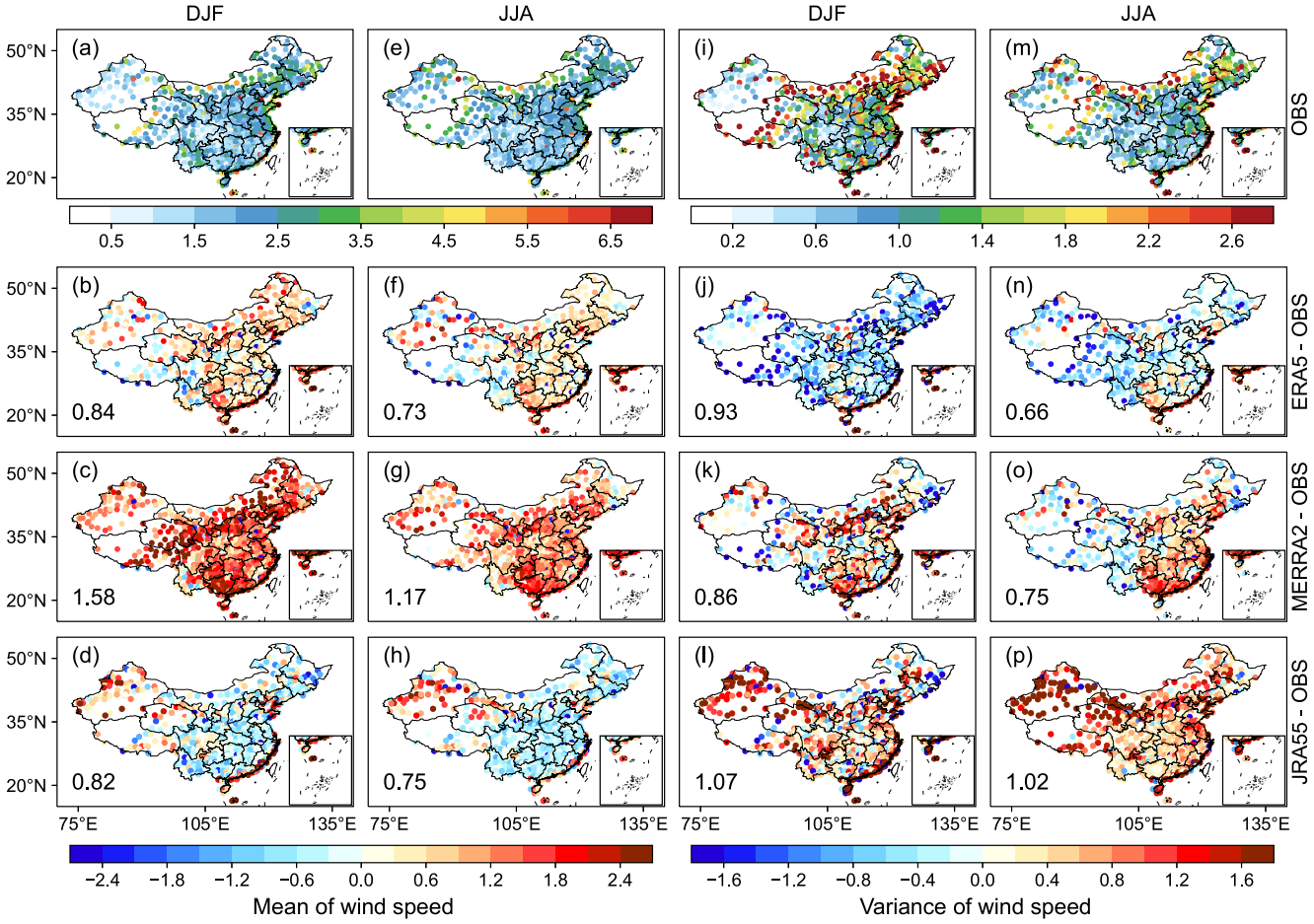


Fig. 1. Spatial distribution of the (a, e) mean and (i, m) variance of the observed SWS over China in winter and summer, and the differences between the (b, f, j, n) ERA5, (c, g, k, o) MERRA2, and (d, h, l, p) JRA-55 reanalyses and observations. Positive values indicate the reanalysis provides a wind speed or variance greater than observed, and the RMSE value is shown in the bottom left of each panel. Units: m s^{-1}.

summer (first row), along with the differences between reanalyses and observations (second to fourth rows). Positive (negative) values mean the wind speed is larger (smaller) in reanalyses than in observations (Fig. 1(b–d, f–h)). From top to bottom are the observations, and differences compared with ERA5, MERRA2, and JRA-55, respectively. The observed SWSs are mostly concentrated in the range of 1–3 m s^{-1}, with high wind speeds (> 3 m s^{-1}) located in the western and northern parts of China, and even higher wind speeds (> 5 m s^{-1}) observed over the high mountains. In contrast, wind speeds in central and southern China are generally weak (< 2.5 m s^{-1}). There are no significant differences between summer and winter. While all three reanalyses successfully capture the spatial pattern of the wind speed as in observations, there are notable differences in magnitude. Compared to the observations, ERA5 and MERRA2 tend to systematically overestimate the SWS, with deviations ranging from 0.3 to 0.9 m s^{-1} for the former to >1.5 m s^{-1} for the latter. In contrast, JRA-55 underestimates the SWS in most parts of China, with deviations mostly in the range of 0.6 m s^{-1}. In view of the spatially averaged root-mean-square error (RMSE) labeled in the bottom left corner of each plot, ERA5 and JRA-55 show comparable performance, and both outperform MERRA2. To explore the intraseasonal variability of SWS, the right two columns of Fig. 1 show the spatial distribution of the seasonal variance of SWS. The observations exhibit larger variance of SWS in northeastern China, with an amplitude greater than 2.2 m s^{-1}. The variance of SWS is generally smaller in summer than in winter. Compared to observations, ERA5 and JRA-55 underestimate the variance of the SWS, with differences mostly in the range of 1.2 m s^{-1}, while MERRA2 tends to overestimate the variance of SWS. In terms of the spatially averaged RMSE, MERRA2 performs best in winter with an average RMSE of 0.86 m s^{-1}, whereas ERA5 performs best in summer with an average RMSE of 0.66 m s^{-1}.

3.2. SWSs over the western North Pacific

Fig. 2 presents the spatial distribution of the seasonal means and variances of SWS over the western North Pacific (WNP). Observed wind speeds are remarkably larger than those over land, especially in winter, with wind speeds exceeding 9 m s^{-1} in most areas. In comparison with the observations, ERA5 and MERRA2 underestimate the SWS, with the deviations ranging from 0.2 to 1.6 m s^{-1}, while JRA-55 slightly overestimates the SWS. Most strikingly, the biases in the three reanalysis products are of opposite sign to those on land and are relatively smaller than those on land. The reason for this is that all three reanalyses used in this study assimilate some observations of surface oceanic winds in their assimilation models, whereas the SWS over land is entirely parametrized in planetary boundary layer schemes based on surface characteristics, stability indices, and the lowest model level winds (Ramon et al., 2019). Another difference from the terrestrial situation is that SWS over the ocean has a distinct seasonal variation, with higher winds in winter and relatively lower winds in summer, partly due to the lowering of the height of the planetary boundary layer in summer, which decouples upper atmospheric levels and their associated winds from the surface. All three reanalyses show positive deviations from observations, and the biases are mostly within a small range of 0.4 m s^{-1}. With respect to the variance of SWS, larger values are observed over the northern and southern parts of the ocean in winter, and near the southern offshore in summer. All reanalyses except JRA-55 underestimate the variance of

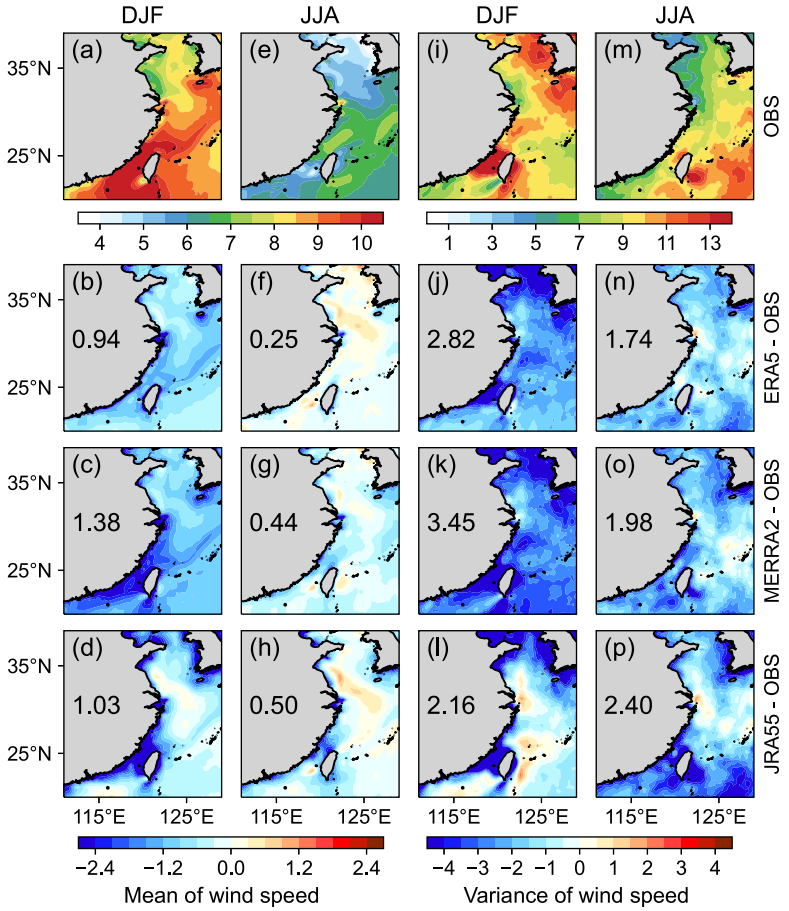


Fig. 2. Spatial distribution of the (a, e) mean and (i, m) variance of the observed SWS over the WNP in winter and summer, and the differences between the (b, f, j, n) ERA5, (c, g, k, o) MERRA2, and (d, h, l, p) JRA-55 reanalyses and observations. Positive values indicate the reanalysis provides a wind speed or variance greater than observed, and the RMSE value is shown in the center left of each panel. Units: m s^{-1}.

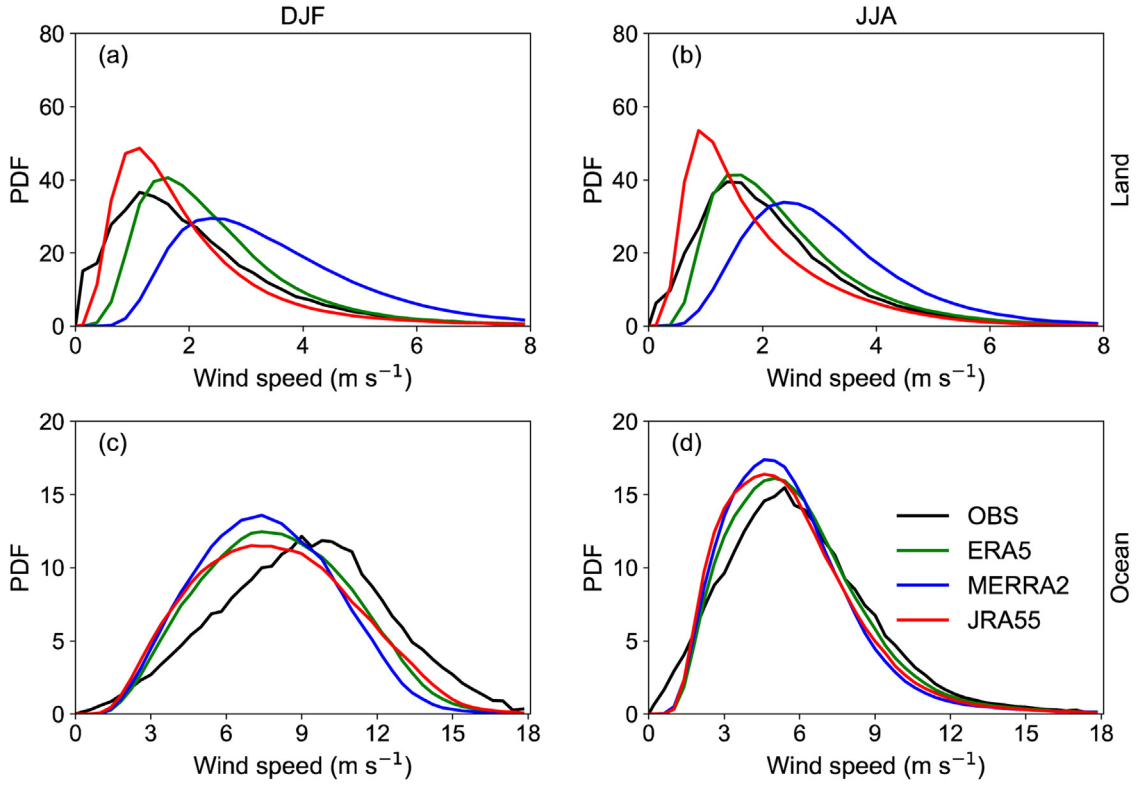


Fig. 3. PDFs of SWSs for both observations (black line) and the ERA5 (green line), MERRA2 (blue line), and JRA-55 (red line) reanalyses over (a, b) China ("Land") and (c, d) the WNP ("Ocean") in winter and summer.

SWS, particularly in winter, with differences mostly between −4 and −1 m s^{-1}. In terms of the spatially averaged RMSE, JRA-55 performs best in winter, followed by ERA5 and then MERRA2. In summer, ERA5 performs best, followed by MERRA2 and then JRA-55.

To further explore the variability of SWS, Fig. 3 displays the probability distribution functions (PDFs) of SWSs, which are divided into 50 bins of equal width. The observed distribution appears to be single peaked, obeying a Gaussian distribution over the ocean and a Gamma distribution with positive skewness over land. While the PDF characteristics (shape and width) in all three reanalyses bear a close resemblance to the observations over the ocean, considerable differences are observed over land. In comparison with the observation, MERRA2 shows a significant PDF rightward shift, indicating that its first-order statistical distance is the largest of the three, in line with a larger value of SWS (Fig. 1(c, g)). On the contrary, JRA-55 shows a leftward shift, indicating that its first-order statistical distance is the smallest of the three, in line with a smaller value of SWS (Fig. 1(d, h)). Furthermore, MERRA2 underestimates the peak value, while JRA-55 overestimates it, compared to the observation. ERA5 is the only one that produces PDF features close to the observation. Given that wind power density is highly nonlinearly related to SWS ($\propto V^3$), differences in the PDF of SWS can lead to significant biases in wind power density, even if the seasonal means are unbiased. This highlights the importance of accurate representation of short-timescale SWS in numerical weather prediction models for better forecasting the wind power density.

4. Trend analysis of SWS

Fig. 4 illustrates the spatial distribution of the SWS trend over China and the WNP for both observations and the three reanalyses. Although there are sporadic positive trends in central and southern China, negative trends prevail in most parts of China, with a typical value of −0.2 m s^{-1}/10 yr. The spatially averaged trend is −0.08 m s^{-1}/10 yr, in agreement with many previous studies showing a decline of about 0.3 m s^{-1} for SWS over land in the northern midlatitudes during the past 30 years (Bichet et al., 2012). The decrease in SWS is partly due to increased surface roughness lengths as a result of urbanization and/or afforestation (Pryor et al., 2009; Guo et al., 2011). Changes in atmospheric circulation due to the meridional temperature gradient induced by global warming may also partly explain the observed wind stilling (Klink, 1999; Zhou et al., 2017). The reanalyses show very different characteristics compared to the observation. ERA5 shows no significant trend over land, as the value is mostly <0.01 m s^{-1}/10 yr. MERRA2 successfully captures the negative trend as in the observations, yet its magnitude is obviously underestimated. JRA-55 shows a negative trend similar to that in the observations in eastern China, but erroneously produces a positive trend in northwestern China. Regarding SWS trends over the ocean, the observation shows a positive trend in most parts of the WNP, with values greater than 0.2 m s^{-1}/10 yr (Fig. 4(h)). The spatially averaged trend is 0.09 m s^{-1}/10 yr, which may be related to the strengthening of the winds as a result of increased sea surface temperature (Zheng et al., 2016). Such a positive trend is marginally captured by ERA5. MERRA2 exhibits a significant negative trend in most of the regions, with a spatially averaged trend of −0.17 m s^{-1}/10 yr, contrary to the observations. Only JRA-55 shows a positive trend comparable to observations in most areas, although the spatially averaged trend is underestimated by almost half. The above analysis suggests that while reanalyses with assimilated surface wind observations can well represent seasonal means of SWS, it remains a difficult challenge for assimilated models to accurately represent long-term trends of SWS.

To understand the extent to which the SWS trend can be attributed to large-scale circulations, we also show in Fig. 4 the wind speed trends at the native level of 850 hPa, which has been used to investigate the role of large-scale circulation in wind speed trends (Chen et al., 2013; Nchaba et al., 2017; Troccoli et al., 2012). As can be seen, there is a similarity between the SWS trends at 10 m and 850 hPa, with the average

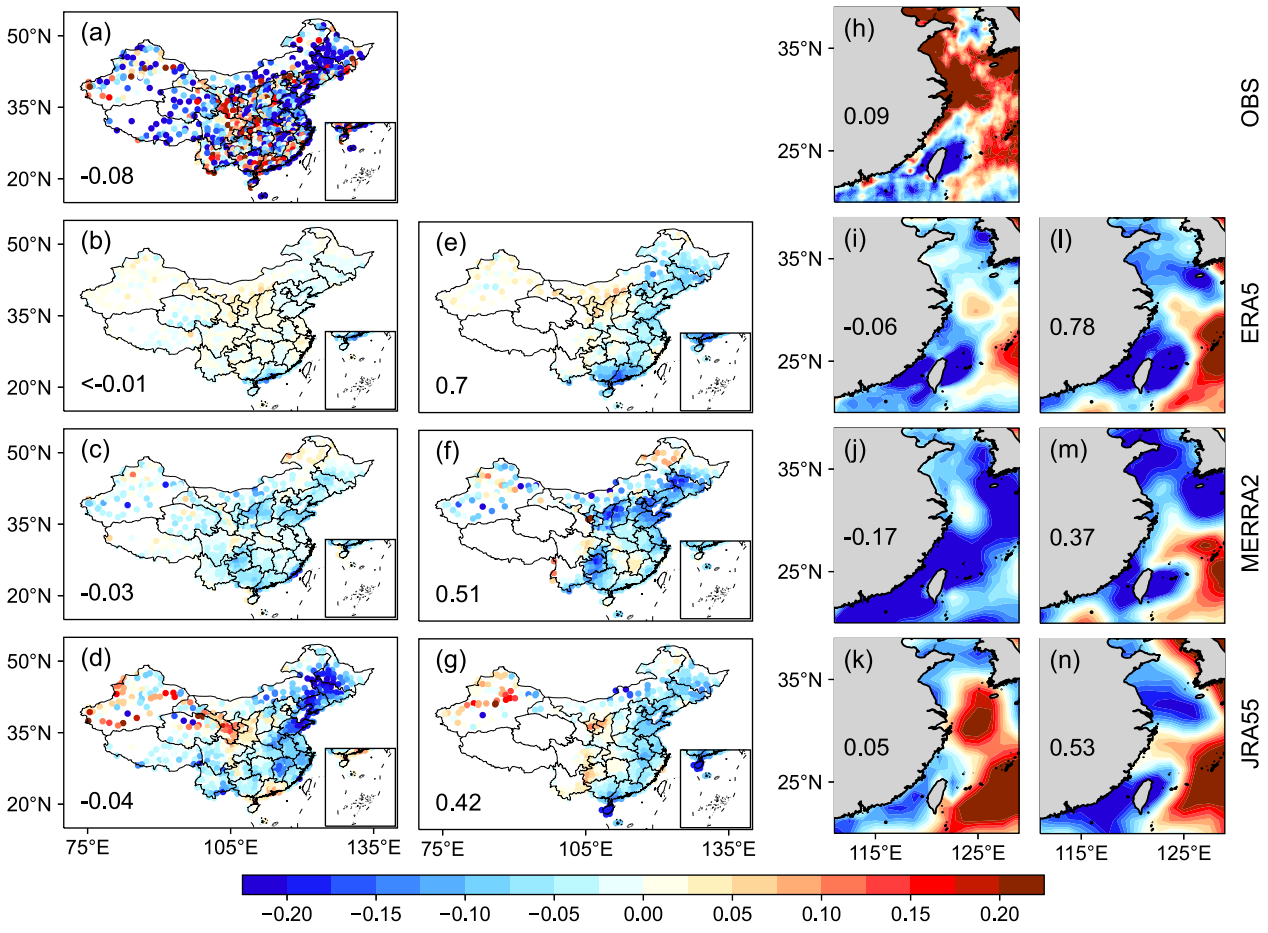


Fig. 4. Linear trend of SWSs for (a, h) observations, (b, e, i, l) ERA5, (c, f, j, m) MERRA2, and (d, g, k, n) JRA-55. The first and third columns are for the spatial mean value of SWS, while the second and fourth columns are for the wind speed at 850 hPa, where the average correlation between the SWS trends at 10 m and 850 hPa are shown by the numbers. Units: m s^{-1}/10 yr.

correlation exceeding 0.7 for ERA5, and 0.4 for MERRA2 and JRA-55. This suggests there is a strong link between the trend of SWS and that of the large-scale circulation, and that a large part of the SWS trend can be attributed to changes in large-scale circulation. The strengthened impact of internal climate variability (e.g., the Pacific Decadal Oscillation, North Pacific Oscillation, and El Niño–Southern Oscillation) in the recent pronounced warming may further regulate surface wind variation by influencing ocean temperature and atmospheric circulation (Cai et al., 2024; Chen et al., 2024). The above analysis demonstrates that although wind speeds are sensitive to the methodologies used to derive the 10 m wind speed, the long-term trend is largely determined by the large-scale circulation.

5. Conclusion

In this study, the credibility of SWSs in three reanalyses (ERA5, MERRA2, and JRA-55) in East Asia is assessed using both satellite and in-situ observations. The key findings and implications can be summarized as follows:

All three reanalysis datasets can generally capture the spatial pattern of wind speeds but show diversity in terms of wind intensity. On land, ERA5 and MERRA2 overestimate the SWS by about 0.6 and 1.5 m s^{-1}, respectively, whereas JRA-55 underestimates it by about 0.6 m s^{-1}. In view of the spatially averaged RMSE of SWS, JRA-55 and ERA5 show comparable performance, and both outperform MERRA2. The biases over the oceans are opposite to those on land and are relatively small due to the assimilation of observations of oceanic surface winds. Overall, JRA-55 and ERA5 offer better estimates of seasonal means and variances of SWS than MERRA2. Further investigation reveals that MERRA2 produces PDFs with a significant rightward shift, whereas JRA-55 shows a leftward shift. Only ERA5 produces PDFs with characteristics close to those observed.

The observed SWS shows a negative trend of −0.08 m s^{-1}/10 yr over China and a positive trend of 0.09 m s^{-1}/10 yr over the WNP. The reanalyses show very different characteristics compared to the observation. ERA5 shows no significant trend in China. MERRA2 captures the negative trend as in observations, yet the magnitude is obviously underestimated. Only JRA-55 shows a negative trend similar to that in the observations. Over the ocean, the positive trend in observations is successfully captured by JRA-55, but only marginally captured by ERA5. MERRA2 exhibits a significant negative trend in most regions, with a spatially averaged trend of −0.17 m s^{-1}/10 yr, contrary to the observations. Comparison of the wind speed trends between 10 m and 850 hPa shows strong similarities, indicating there is a link between the trend of SWS and that of the large-scale circulation, and that a large part of the SWS trend can be attributed to changes in large-scale circulations.

Data availability

All satellite and reanalysis datasets used in this study are available to the public. The QuikSCAT and ASCAT satellite products can be downloaded from https://data.remss.com/. The ERA5 reanalysis is available from https://cds.climate.copernicus.eu/. The MERRA2 reanalysis

is available from https://goldsmr4.gesdisc.eosdis.nasa.gov/. The JRA-55 reanalysis is available from https://data.rda.ucar.edu/.

Funding

This work was jointly supported by the National Natural Science Foundation of China [grant numbers 42361144708, 42205041, and 42175165], a scientific research project of the Shanghai Investigation, Design and Research Institute Co., Ltd. [grant number 2023CN(83)-001], and the National Key Scientific and Technological Infrastructure project "Earth System Science Numerical Simulator Facility" (EarthLab).

Acknowledgements

The author thanks the two anonymous reviewers for their constructive comments that helped to clarify and improve the original paper.

References

Bichet, A., Wild, M., Folini, D., Schär, C., 2012. Causes for decadal variations of wind speed over land: Sensitivity studies with a global climate model. Geophy. Res. Lett. 39 (11), L11701.

Cai, Q., Chen, W., Chen, S., Xie, S., Piao, J., Ma, T., Lan, X., 2024. Recent pronounced warming on the Mongolian Plateau boosted by internal climate variability. Nat. Geosci. 17 (3), 1–8.

Cannon, D.J., Brayshaw, D.J., Methven, J., Coker, P.J., Lenaghan, D., 2015. Using reanalysis data to quantify extreme wind power generation statistics: A 33 year case study in Great Britain. Renew. Energ. 75, 767–778.

Chen, L., Li, D., Pryor, S.C., 2013. Wind speed trends over China: Quantifying the magnitude and assessing causality. Int. J. Climatol. 33 (11), 2579–2590.

Chen, S., Chen, W., Xie, S., Yu, P., Wu, R., Wang, Z., Lan, X., Graf, H.F., 2024. Strengthened impact of boreal winter North Pacific Oscillation on ENSO development in warming climate. npj Clim. Atmos. Sci. 7 (1), 69.

Das, A., Roy, S.B., 2024. JRA55 is the best reanalysis representing observed near-surface wind speeds over India. Atmos. Res. 297, 107111.

Dickinson, S., Kelly, K.A., Caruso, M.J., Mc Phaden, M.J., 2001. Comparisons between the TAO buoy and NASA scatterometer wind vectors. J. Atmos. Ocean. Technol. 18 (5), 799–806.

Fischedick, M., Schaeffer, R., Adedoyin, A., Akai, M., Bruckner, T., Clarke, L., Krey, V., et al., 2011. Mitigation potential and costs. In: Edenhofer, O., Pichs-Madruga, R., Sokona, Y., Seyboth, K., Matschoss, P., Kadner, S., Zwickel, T., et al. (Eds.), IPCC Special Report on Renewable Energy Sources and Climate Change Mitigation. Cambridge University Press, Cambridge, United Kingdom and New York, NY, USA, pp. 791–864.

Gelaro, R., McCarty, W., Suárez, M.J., Todling, R., Molod, A., Takacs, L., Randles, C.A., et al., 2017. The modern-era retrospective analysis for research and applications, version 2 (MERRA-2). J. Clim. 30 (14), 5419–5454.

Goutham, N., Alonzo, B., Dupré, A., Plougonven, R., Doctors, R., Liao, L., Mougeot, M., et al., 2021. Using machine-learning methods to improve surface wind speed from the outputs of a numerical weather prediction model. Boundary-Layer Meteorol. 179, 133–161.

Guo, H., Xu, M., Hu, Q., 2011. Changes in near-surface wind speed in China: 1969–2005. Int. J. Climatol. 31 (3), 349–358.

Hersbach, H., Bell, B., Berrisford, P., Hirahara, S., Horányi, A., Muñoz-Sabater, J., Nicolas, J., et al., 2020. The ERA5 global reanalysis. Q. J. R. Meteorol. Soc. 146 (730), 1999–2049.

Klink, K., 1999. Trends in mean monthly maximum and minimum surface wind speeds in the coterminous United States, 1961 to 1990. Clim. Res. 13 (3), 193–205.

Kobayashi, S., Ota, Y., Harada, Y., Ebita, A., Moriya, M., Onoda, H., Onogi, K., et al., 2015. The JRA-55 reanalysis: General specifications and basic characteristics. J. Meteorol. Soc. Jpn. 93 (1), 5–48.

Miao, H., Wang, X., Liu, Y., Wu, G., 2019. An evaluation of cloud vertical structure in three reanalyses against CloudSat/cloud-aerosol lidar and infrared pathfinder satellite observations. Atmos. Sci. Lett. 20 (7), e906.

Miao, H., Dong, D., Huang, G., Hu, K., Tian, Q., Gong, Y., 2020. Evaluation of northern hemisphere surface wind speed and wind power density in multiple reanalysis datasets. Energy 200, 117382.

Minola, L., Zhang, G., Ou, T., Kukulies, J., Curio, J., Guijarro, J.A., Deng, K.Q., et al., 2024. Climatology of near-surface wind speed from observational, reanalysis and high-resolution regional climate model data over the Tibetan Plateau. Clim. Dyn. 62 (2), 933–953.

Nchaba, T., Mpholo, M., Lennard, C., 2017. Long-term austral summer wind speed trends over southern Africa. Int. J. Climatol. 37 (6), 2850–2862.

Pryor, S.C., Barthelmie, R.J., Young, D.T., Takle, E.S., Arritt, R.W., Flory, D., Gutowski Jr., W.J., et al., 2009. Wind speed trends over the contiguous United States. J. Geophy. Res. Atmos. 114 (D14).

Ramon, J., Lledó, L., Torralba, V., Soret, A., Doblas-Reyes, F.J., 2019. What global reanalysis best represents near-surface winds? Q. J. R. Meteorol. Soc. 145 (724), 3236–3251.

Ray, S., Swain, D., Patidar, G., Jayaram, C., 2022. Comparison of SCATSAT-1 swath data with global in situ buoy winds. Geocarto Int. 37 (26), 11068–11087.

Ricciardulli, L., Manaster, A., 2021. Intercalibration of ASCAT scatterometer winds from MetOp-A,-B, and-C, for a stable climate data record. Remote Sens. 13 (18), 3678.

Vishnu, S., Francis, P., 2014. Evaluation of high-resolution WRF model simulations of surface wind over the west coast of India. Atmos. Ocean. Sci. Lett. 7 (5), 458–463.

Torralba, V., Doblas-Reyes, F.J., Gonzalez-Reviriego, N., 2017. Uncertainty in recent near–surface wind speed trends: A global reanalysis intercomparison. Environ. Res. Lett. 12 (11), 114019.

Troccoli, A., Muller, K., Coppin, P., Davy, R., Russell, C., Hirsch, A.L., 2012. Long-term wind speed trends over Australia. J. Clim. 25 (1), 170–183.

Wang, X., Zhang, M., 2024. Convectively coupled Rossby-Gravity waves in a field campaign: How they are captured in reanalysis products. Atmos. Sci. Lett. 25 (4), e1206.

Wu, J., Zha, J., Zhao, D., Yang, Q., 2018. Changes in terrestrial near-surface wind speed and their possible causes: An overview. Clim. Dyn. 51 (5), 2039–2078.

Zheng, C.W., Pan, J., Li, C.Y., 2016. Global oceanic wind speed trends. Ocean Coast. Manag. 129, 15–24.

Zheng, F., Du, J., Zhu, J., 2009. A reconstructed wind stress dataset for climate research over the tropical pacific during a 153-year period. Atmos. Ocean. Sci. Lett. 2 (5), 277–283.

Zhou, B., Zheng, F., Zhu, J., 2017. Analysis of the interannual variations and influencing factors of wind speed anomalies over the Beijing–Tianjin–Hebei region. Atmos. Ocean. Sci. Lett. 10 (4), 312–318.